Cell Tiss. Res. 183, 221–237 (1977)

Cell and Tissue Research

Quantitative Autoradiographic Light- and Electron Microscopic Studies on the Retinohypothalamic Connections in the Rat

J.K. Mai and E. Junger

C. u. O. Vogt – Institut für Hirnforschung der Universität Düsseldorf und Diabetesforschungsinstitut an der Universität Düsseldorf, Biochemische Abteilung, Düsseldorf, Bundesrepublik Deutschland

Summary. Light microscopic autoradiography performed subsequent to intraocular injection of ^{3}H-leucine revealed silver grains (SG) above axons of the optic tract which could be followed into the ventral and caudal portion of the suprachiasmatic nuclei (SCN) and above the contralateral anterior hypothalamic nucleus (AHN). By high resolution photometric measurement and computer processing the labelled areas were analysed, thus yielding statistical data of the relative grain distribution. The highest SG density was found in the ventrolateral part of both SCN (SCvl), confirming earlier reports concerning retinohypothalamic connections. That area exhibiting a cytoarchitecture different from the remaining nucleus was traversed, however, by numerous labelled axons. In the caudal part of both SCN a specific projection field of retinal fibres could be located. Here, almost no traversing fibres contribute to the rather circumscribed marked area. In the ventral part of the contralateral AHN, diffuse labelling well above background levels could be observed. Distinction between bypassing and terminating fibres within the SCvl could not be made using light microscopy. Analysis of SG distribution of the SCvl with electron microscopic autoradiography revealed a specific localization of SG within presynaptic terminals containing clear vesicles and pale mitochondria.

Key words: Visual system (Rat) – Autoradiography – Quantitative analysis – Suprachiasmatica nucleus – Ultrastructure.

Send offprint requests to: Dr. J.K. Mai, C. u. O. Vogt – Institut für Hirnforschung der Universität Düsseldorf, Universitätsstr. 1, D-4000 Düsseldorf, Federal Republic of Germany

Acknowledgements: The authors are indebted to Professor A. Hopf for his generous support and valuable help, to Professor E. Reale for help in cytoarchitectural evaluation, to Professor H.J. Jesdinski and Dr. O. Richter for advice in statistical analysis, and to Mrs. I. Haas for expert help in computer processing. The technical assistance of Mrs. I. Latka and Mrs. M. Gatzke is greatly appreciated

Introduction

Results of previous investigations using autoradiography have supported the existence of a direct retinal connection with the suprachiasmatic nucleus (SCN) of the medial hypothalamus (for review, see Mai, 1976). In contrast to previous schemata which illustrate the SCN differentiating from subjacent chiasmatic axons (Palkovits et al., 1974), the SCN lies embedded within the optic chiasma (Bellonici, 1888; Hayhow et al., 1960; 1962). Therefore, it is impossible to differentiate the axonal terminals from fibres en passage. As is the case with virtually all nuclear, non-cortical cell groups, it is impossible to distinguish light microscopically terminals or synapses en passant (Rosenstein and Leure-du-Pree, 1976) from obliquely sectioned non-synaptic axonal processes.

The aim of the present study, was to confirm synaptic sites of retinal origin in the ventrolateral part of the SCN (SCvl) by employing electron microscopic autoradiography (EM-ARG). Specimens for EM-ARG were examined subsequent to a preliminary survey of the entire brain by quantitative light microscopic autoradiography (LM-ARG).

Material and Methods

The experiments were carried out on 69 male albino rats (Wistar strain, weight 270–330 g). 64 rat brains were used for light microscopic evaluation.

Application of the Tracer. The animals were lightly anaesthesised with methoxyfluorane (Penthrane, Abbott). Between 25 µl and 135 µl of an aqueous solution of L-(4.5-^{3}H)leucine (S.A. 30 Ci/mmole = µCi/µl, Amersham Buchler) was injected via the superior corneal limbus of the right eye into the vitreous body. The injection was made using a Hamilton microsyringe attached to a stereotaxic apparatus (Stoelting) and lasted for at least 1 min.

Preparation of the Tissue. After survival times ranging from $2^1/_2$ h to 30 days for light and 12 to 24 h for electron microscopic investigation, the animals were perfused according to the method of Schultz and Case (1970) with 0.5 ml (10,000 USP-U) sodium heparinate, 50 ml Ringer's solution and 500 ml 4% 0.1 M phosphate-buffered formaldehyde (pH 7.4, 1600 mosmol) for a period of approximately 30 min at room temperature and at a pressure of 110 mmHG. Immediately after perfusion the rats were decapitated. The brains and eyes were quickly removed.

Histological Preparation for Light Microscopy. The brains were left in the fixative for at least 24 h. They were embedded in paraffin and sectioned at 17 µm, either in the horizontal, oblique horizontal, coronal or sagittal plane.

Autoradiography. After removal of paraffin and hydration, sections were prepared for autoradiography with Kodak NTB-2 emulsion according to the procedure of Kopriwa and Leblond (1962) and Cowan et al. (1972). Following an exposure of between 4 and 20 weeks, the specimens were developed in Kodak Dektol for $1^1/_2$ min at 17° C, rinsed in water, fixed in Acidofix (Agfa-Gevaert) for 10 min and afterwards washed in deionized water for 15 min. The sections were analysed either stained with cresyl violet or unstained by reflected bright-field illumination. Quantitative measurements performed prior to staining the sections prevented artefacts by tissue reflection.

Analysis. The suprachiasmatic nuclei and adjacent areas were scanned in raster pattern at actual stage steps of 10 µm. Using reflected bright-field illumination and a magnification of × 1000 the reflection was measured by a Leitz-photometer unit as described by Dörmer (1972). Data, provided by the photomultiplier as relative values of the number of SG, were digitized and stored on magnetic tape to-

gether with the coordinates of the measured rectangular area, to allow detailed analysis of a subsector and, moreover, to permit three-dimensional evaluation of serial sections in a future study. The stage movement was initiated by pushing a button on a keyboard displaying different code numbers which permit the investigator to encode the morphological landmarks as well as artefactual counts. The magnetic tape was processed and plotted with the aid of a computer (Siemens 4004/45). Thresholds of graphic display could be chosen freely with punched cards.

Processing for Electron Microscopy. The perfused brains were cut into 1 mm slices (frontal). Right and left hemispheres were separated and the SCN carefully excised, including parts of the optic chiasma (CO) and the third ventricle. By morphological characteristics and topographical arrangement of the latter structures, oriented embedding and sectioning were facilitated. Tissue blocks were additionally fixed by immersion in 4% formaldehyde (see above) for 90 min. After rinsing in 0.1 M phosphate buffer (pH 7.4, 225 mosmol) tissue blocks were postfixed in 2% OsO_4 (pH 7.4, 350 mosmol) for 2 h, dehydrated in graded ethanol and embedded in Epon 812.

Autoradiography. For autoradiography the total region of the contralateral SCN was sectioned stepwise. One step included three semithin sections, approximately 2.5 µm thick, and 30 ultrathin sections, interference colour gold, equivalent to a section thickness of 0.12 µm. Between each step 17 semithin sections were discarded. Semithin sections were mounted on glass slides, ultrathin sections on collodion coated slides. They were subsequently covered with a 50–100 Å carbon layer. Ilford L 4 emulsion was applied by the dropper method (Salpeter and Bachmann, 1964). The emulsion was diluted until a purple monolayer covered that area on which the sections have been placed. After exposure for 10 to 30 weeks at 4° C the specimens were developed in Microdol X for 3 min at 23° C, passed through a stop bath of acetic acid and fixed in 20% sodium thiosulfate. Semithin sections were stained with toluidine blue and examined in the light microscope.

Serial sections for electron microscopy were stripped onto a water surface. Sections were mounted on 400 mesh copper grids and stained with lead citrate according to Venable and Cogeshall (1965).

Analysis. Overall grain distribution was obtained by scanning the total section area at low electron microscopic magnification (× 2000). Section domains, exhibiting the highest grain density, were selected and in these domains all grains were recorded at × 5000. For further evaluation prints enlarged three times were used. In order to localise the sites of disintegration, probability circles of 50%, 66% and 90% were used. Size of the circles was estimated from the half distance (HD) value for a point source of tritium radiation as calculated by Bachmann et al. (1968). According to our geometrical specimen parameters, the HD value should be approximately 1700 Å. The percentage of "exclusively" and "shared" grains was determined, using synaptic terminals and "other" structures as separate entities. According to the definition of Nadler (1971), "exclusive" means that only one item is observed within the probability circle. "Shared" means, in this context, that in addition to synaptic terminals at least one other biological structure is visible within the circle. The considerable number of shared grains necessitated weighing of the structures within the circles. Therefore, the partial areas of synaptic terminals were determined within circles for both, 66% and 90% probability. Experimentally observed label distribution was compared with a random distribution using χ^2-test for significance. For details, see Table 1. Measurements of areas were carried out with an electronic planimeter (MOP/AM 01 Kontron).

Results

Light Microscopy. Label beyond the chiasmatic level was evident in all brains obtained 12 and more hours after injection of tritiated leucine. At this time the hypothalamic area as well as the primary and accessory optic centres were heavily labelled.

Label above background level overlying the parastriate- or parahippocampal cortex was not observed. Variation of survival times, of the amount of injected label, of the numbers and intervals of injections in the same animals and of the exposure

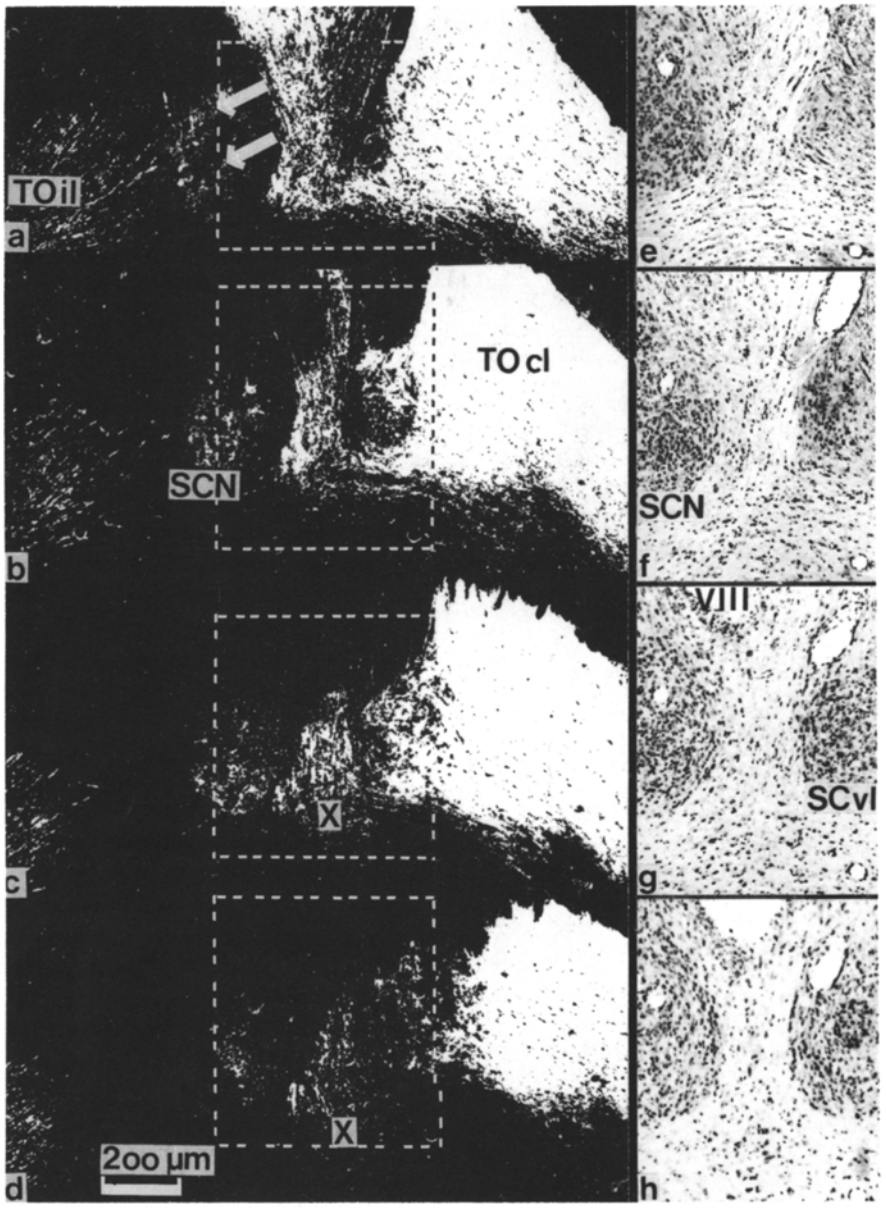

Fig. 1 a–h. Horizontal sections, mounted from ventral to dorsal, through the SCA. **a–d** Dark field photomicrographs showing the course of labelled optic nerve fibres after intravitreous injection of 25 µl tritiated leucine 10 days before sacrifice. Exposure time was 7 weeks. The ipsilateral SCN appears connected with the labelled surrounding tissue only at the ventral-most part (*arrows* in Fig. 1 a). **e–h** Photomicrographs of the same Nissl-stained sections by transmitted light of the area indicated in a–d by dotted lines. Abbreviations used in this and the following figures: *AHN* anterior hypothalamic nucleus; *BFI* bright field illumination; *CO* optic chiasma; *SCA* suprachiasmatic area; *SCN* suprachiasmatic nucleus; *SCNcl* suprachiasmatic nucleus contralateral to the injected eye; *SCNil* ipsilateral SCN; *SCvl* ventrolateral part of SCN; *SGS* stratum griseum superficiale of superior colliculus (*CS*); *SO* stratum opticum of CS; *TO* optic tract; *TOcl* optic tract contralateral to the injected eye; *TOil* optic tract of the ipsilateral side; *V III* third ventricle; *X* medial bundle of optic late crossing fibres; *aaot* anterior accessory optic tract; *cht* medial cortico-hypothalamic tract; *stp* precommissural component of the stria terminalis

times did not essentially influence the patten of grain distribution but only the concentration of SG distribution. Augmentation of label, enhanced especially by increasing exposure time, facilitated photometric evaluation of autoradiographs. Therefore, all the plots obtained are directly comparable and give a reliable indication of the relative number of fibres within the areas studied as long the background label is calculated.

Figures 1 and 2 show consecutive horizontal sections through the suprachiasmatic region (SCA), together with the graphic representations of photometric measurements from an animal surviving 13 days. The grain densities of the various structures of interest are documented. The exact demarkation of the unlabelled blood vessels shows that diffusion, redistribution or translocation of radioactive markers during tissue preparation were insignificant as factors influencing quantitation. The compact arrangement of labelled nerve fibres in the lateral part of the optic chiasma and tract is in contrast to the loosened and intermingled course of the medially located optic tract fibres. Examining the SCA at various section planes, the intricate topographical relationship between the SCN, embedded in the dorsal "niveau" of the optic chiasma, and the retinal fibres which extend into this area from various sites is easily recognised.

The biconcave-shaped area between both SCN is traversed by numerous late crossing optic tract fibres ("X" in Figs. 1, 2, 3 and 4). Immediately beyond the caudal pole of both nuclei the bulk of these medial coursing fibres turns at almost right angles in an oblique horizontal manner towards the contralateral main optic tract. Some fibres can be followed beneath the ependyma of the supraoptic recess of the third ventricle before rejoining the main tract. Here, the aberrant fibres occupy a medial position and can be followed to the anterior accessory optic tract.

The ipsilateral SCN is easily distinguished on dark-field illuminated photographs. It appears separated from the surrounding marked structures, connected with the CO and the optic tract only at the ventral-most level by strands of SG (arrows in Fig. 1 a). The shift of radioactive label to the posterior part of the SCN at higher levels is documented.

The contralateral SCN, on the contrary, exhibits much more labelling, the highest SG-concentration to be found in the ventro-lateral position of the anterior and medial parts of the nucleus. The optic fibres traversing this ventro-lateral area are so numerous that the nuclear mass and optic tract, easily distinguished using transmitted light, cannot be separated on dark field illuminated autoradiographs. As can be seen in Figure 3 this heavily labelled area is characterised by a cell type very different from the typical closely clustered SCN-cells with a uniformly dark staining rim of Nissl-substance. The SCvl underlying the dense labelling is composed of rather pale cells, medium in size and polygonal in shape with only few cytoplasmic granules. This type of SCN-cells is very similar to those found in the AHN. In fact, the longer exposed sections through the posterior and dorsal SCA show a labelling of the ventral part of the contralateral AHN. Both labelled areas are separated by the medial cortico-hypothalamic tract (cht) and by the precommissural component of the stria terminalis (stp) (Fig. 3 d). In the posterior part of both SCN the highest SG-concentration is found in a dorsal position. On coronal sections the SG appear well separated from the surrounding labelled structures (Fig. 4). This pattern is produced by the brush-like segregation of fibres

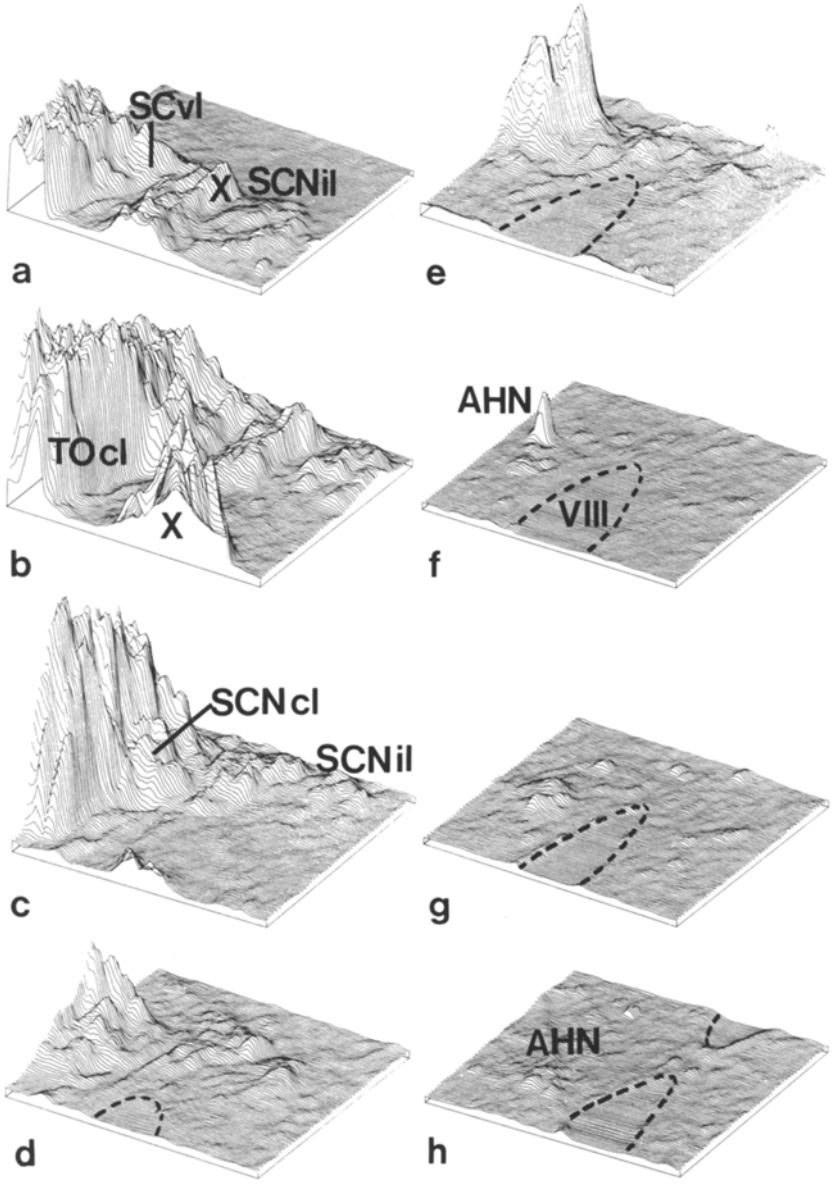

Fig. 2a–h. Graphic representation of SG-densities after photometric measurement of the SCA. The plots, numbered **a–d,** were obtained from the sections shown in Figure 1; the following plots were derived from consecutive sections of the same brain. Before plotting, the data were smoothed by using a moving average with a window size of 5 × 5 measurement values. The graphs were rotated clockwise by 210° corresponding to the angle of view of Figure 1. The square measurement area of the base of every plot covers 1 mm^2. Note that a distance of approximately 70 µm exists between the planes of Figure e and f

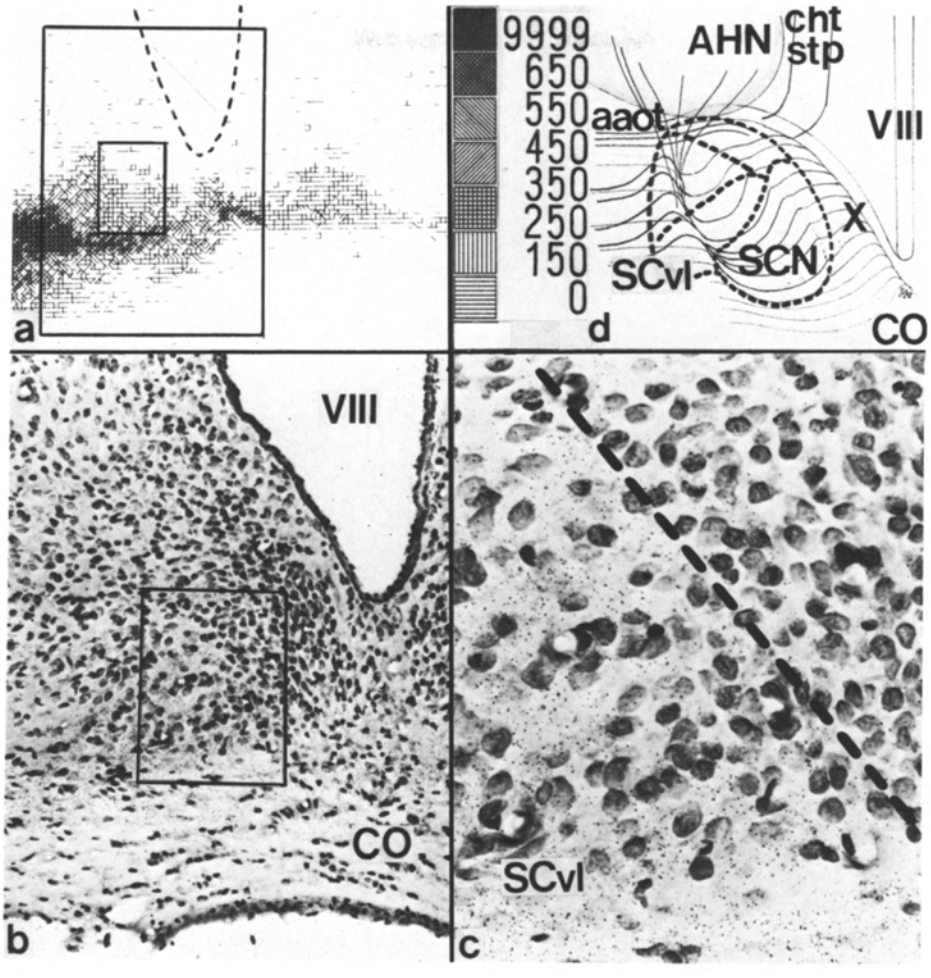

Fig. 3. a Plot, representing photometric measurements of the SG distribution of the medial SCA, shown in coronal section. The original plots obtained after computer processing are drawn in different colours. Blood vessels are indistinguishable from SG in this illustration (both are indicated as black lines) whereas in the original plots these appear as green lines in striking contrast to the different coloured lines representing SG (cf. Fig. 4 b). Values represented by the threshold scale are increased stepwise for the mean values of the background label together with tissue reflection. The areas marked in a, are represented in the photomicrographs by BFI of the same Nissl-stained section (**b, c**). The SG are distributed preferentially over the SCvl exhibiting a different cellular population. b, ×125. c, ×400. The rat was injected with 50 μCi ^{3}H-leucine 11 days before sacrifice. Exposure time was 10 weeks. **d** Schema of the distribution of retinal fibres in relation to the *SCN*. The *SCvl* is traversed by looping retinal fibres, some of which contact the neuropil of the SCvl. Other fibres proceed to the ventral part of the *AHN*

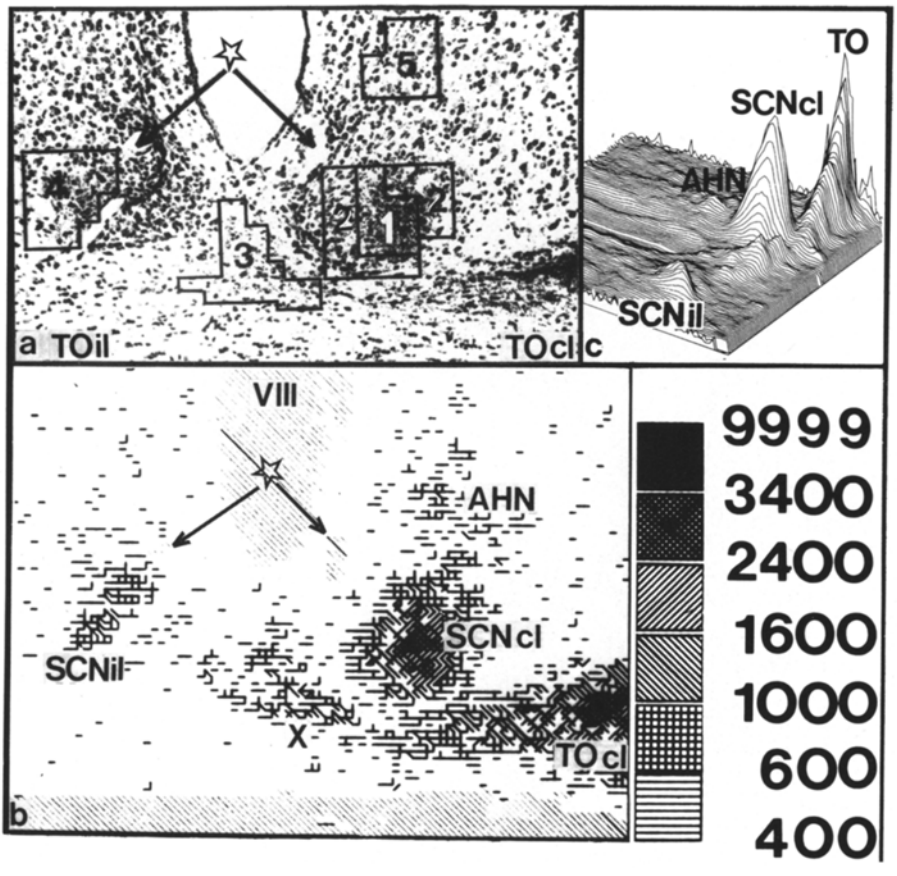

Fig. 4 a–c. Autoradiograph of a coronal section through the SCA and graphic display of the relative SG densities. **a** The labelled caudal area of the SCN is seen clearly separated from the optic tract fibres (*TOil* and *TOcl*). The areas marked *1–5* delineate the regions from which photometric measurement were computed. They were, related to the mean values of the background activities, : 13 : 7 : 5 : 3.5 : 2.5. *Arrows* indicate two blood vessels. **b** Plot representing the photometric measurements of Figure a. The threshold scale at the right indicates photometric values representing the grain density. **c** Presents the three dimensional representation of the relative SG distribution. The base of the plots represents 1 mm. One and eleven days before sacrifice 50 μCi tritiated leucine was injected into the right eye. Exposure time was five months

which can be traced at the base of the SCN before they fan out in an anterior-posterior direction (Fig. 1 a).

Electron Microscopy. The constituent structural features of the SCvl, where grain density was highest (see below), were estimated on a semiquantitative basis from electron micrographs. Analysing a set of random prints, synaptic terminals were found in a random distribution. Eight to 16 synaptic terminals per 140 μm^2 (e.g. the

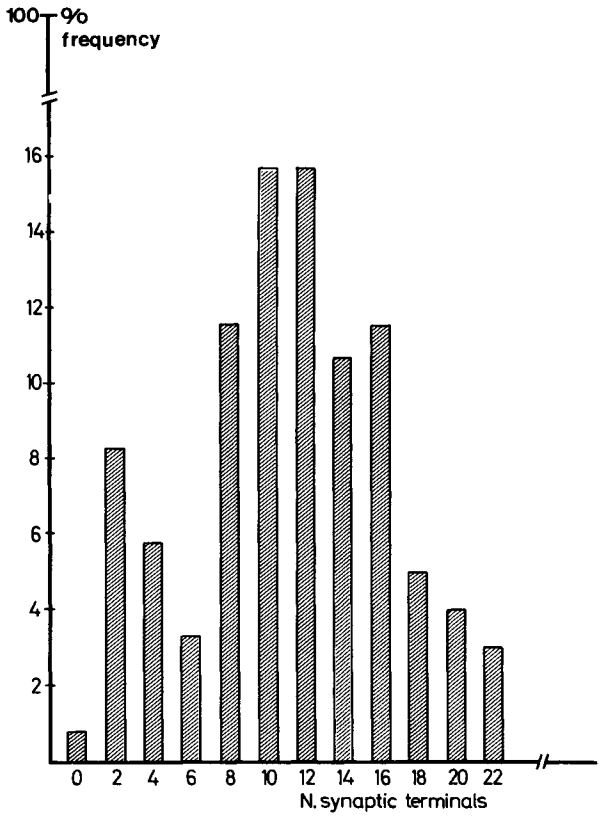

Fig. 5. Relative frequencies of synaptic terminals per 140 μm^2 (= 1 electron micrograph; number of evaluated micrographs = 120)

mean area of one print) were observed in 65 % of all evaluated prints (Fig. 5). In four sections the areas of synaptic terminals were measured and plotted in a histogram (Fig. 6). Approximately 80 % of all terminals were found to be below 1 μm^2 in size and 50 % in the range from 0.3–0.6 μm^2. According to these estimates very low concentrations of radioactivity are to be expected for synaptic terminals at the ultrastructural level. In fact, autoradiographs showed low grain densities (Table 1).

Due to the low amount of incorporated radioactivity, extremely long exposure times, lasting up to 30 weeks, were necessary, which in turn engendered chemography. For this reason, only specimens with an intermediate carbon layer were used. Since chemography differed from one specimen to another, it caused problems in determining background ratios and thus prevented quantitative approach. In this study grain analysis solely served to distinguish between random and nonrandom distribution. Therefore, background ratios were negligible.

In both cases where animals survived for 12 or 24 h, highest grain densities were observed in the SCvl. In this area, which extends 100–150 μm from the CO into the nucleus, the number of grains increased fivefold as compared to other nuclear regions in the same tissue block, sectioned for LM- and EM-ARG. Assigning grains to the structures (Fig. 7) by using a 50 % circle, 15–20 % of the grains were observed

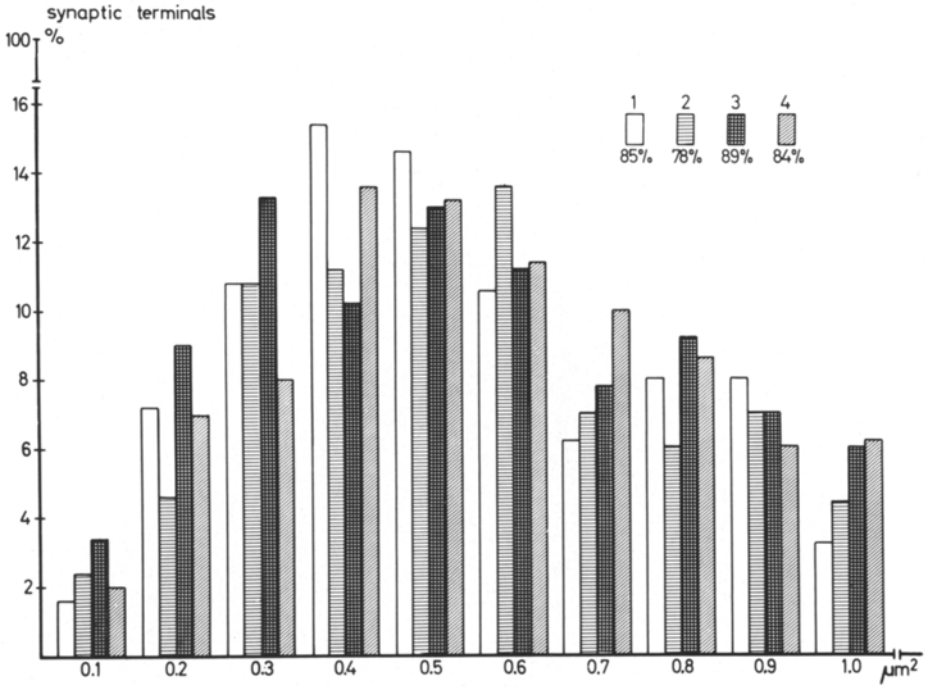

Fig. 6. Frequency distribution of areas of synaptic terminals. Values from four different sections are compared, and are recorded up to 1 µm². The percent of synaptic terminals within this range are given below the section markings. The number of sections corresponds to the notation in Table 1 ($n_1 = 244$, $n_2 = 246$, $n_3 = 299$, $n_4 = 615$)

exclusively overlying synaptic structures, 50–60 % exclusively overlying other structures; 20–30 % were determined to be shared grains. When analysis was based on a 66 % circle, the area of which is virtually in the same range as or larger than of 50 % of the profile areas of synaptic terminals (see Fig. 6), then only 3–5 % exclusive grains were found. The number of shared grains increased to 40–45 %. Using the 90 % circle a further increase of shared grains up to 50–60 % was observed, whereas 35–50 % of the grains exclusively overlie other structures. Among the latter almost 10 % were observed over perikarya, the remainder located over dendrites, axons and glial processes (Fig. 8). The analysis of the labelled synapses showed that SG were most often found overlying presynaptic elements containing clear, loosely packed vesicles and mitochondria with "empty" matrix. These mitochondria frequently revealed a swollen appearance (Fig. 8). Dense core vesicles were not observed in relation to SG (Fig. 9).

As mentioned under Methods, shared grains were further analysed by determining the synaptic areas per circle area. When compared to a random distribution, these values indicate, with a high degree of statistical significance (Table 1), that synaptic terminals are more frequently related to grains than would be expected.

Table 1. Data from eight frontal sections through the ventrolateral part of the contralateral suprachiasmic nucleus. Variable experimental parameters are given in the first part of the table. The second part comprises values of the total evaluated section area, which are obtained by summarising values of the single micrographs

Section Nr.:		1	2	3	4	5	6	7	8
(^{3}H)-leucine administered (μCi)		85	85	85	85	85	85	135	135
survival rate (h)		12	12	12	12	12	12	24	24
exp. time (weeks)		15	23	23	26	26	26	10	10
Evaluation:									
$\sum A_{Sec}$ (μm^2)		1740	2050	2800	3700	3630	4150	4390	2660
$\sum N_G$		35	56	81	88	96	101	85	57
$\sum A_{Sy}$ (μm^2)		90	115	195	250	253	240	190	157
$\sum a_{Sy}$ (μm^2)	90%	11.2	24	36	35	49	36	39	22
	66%	2.8	7.3	9	8				
χ^2_{tot}	90%	3.97*	7.79**	14.02***	10.99***	12.07***	24.91***	37.69***	8.78**
	66%	8.39**	28.29***	28.28***	16.58***				
F	90%	5.22*	7.93*	16.60***	9.71**	13.47***	27.02***	37.88***	7.87*
	66%	4.86*	7.97**	14.92***	11.78**				
k		13	15	21	27	29	28	34	20

* $0.05 \geq P > 0.01$; ** $0.01 \geq P > 0.001$; *** $P \leq 0.001$

Statistical significance was calculated according to:

$$(1) \qquad \chi^2 = \frac{\frac{A_{Sy}}{A_{Sec}} \cdot N_G - \frac{\sum a_{Sy}}{a_C}}{\frac{A_{Sy}}{A_{Sec}} \cdot N_G}$$

$$(2) \qquad F = \frac{\chi^2_{tot} \cdot (k-1)}{\sum \chi^2}$$

(1) is calculated for every micrograph
A_{Sy} = area of synaptic terminals
A_{Sec} = area of the evaluated part of the section
N_G = number of developed grains
a_{Sy} = partial areas of synaptic terminals within each circle
a_C = area of the circle
N_H = numbers of grains which hit synaptic terminals
For χ^2_{tot} values of the single micrographs were summarised
k = number of evaluated micrographs
F is calculated as a measure of heterogeneity

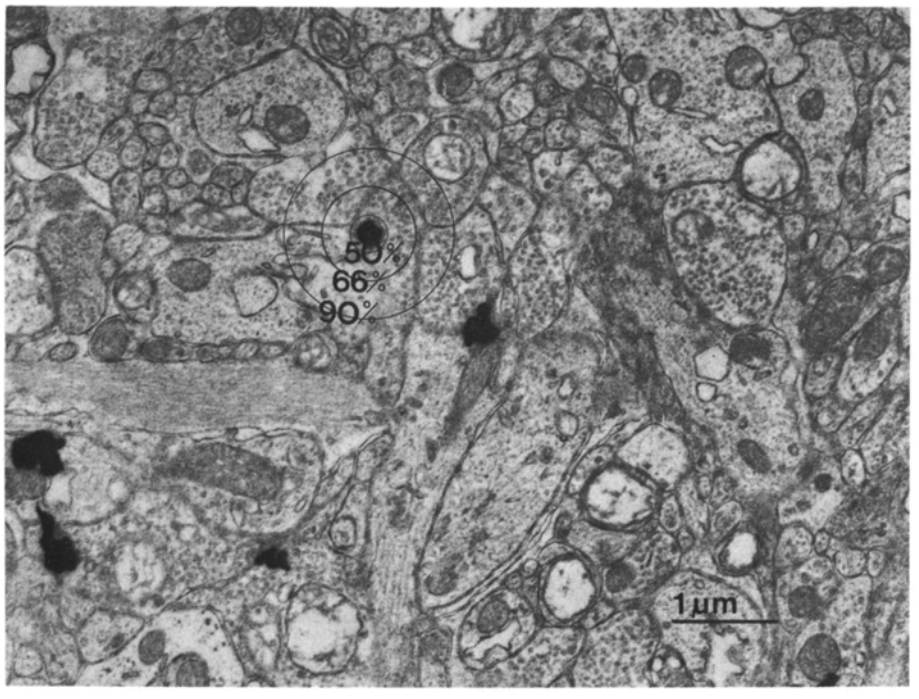

Fig. 7. Electron micrographs from the ventrolateral suprachiasmatic nucleus. Grain distribution is typical in as far as SG are mainly related to presynaptic elements exhibiting mitochondria with pale matrix, irregular cristae and clear, loosely packed vesicles. For demonstration, probability circles of *50%*, *66%* and *90%* used for grain analysis are drawn around one grain

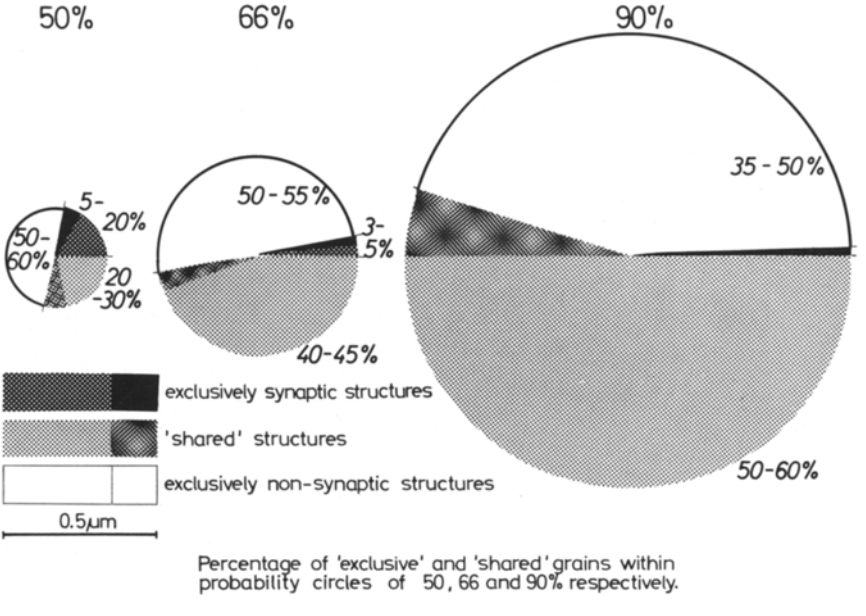

Fig. 8. Representation of the structural elements within probability circles of *50%*, *66%* and *90%*, respectively. For explanation, see text

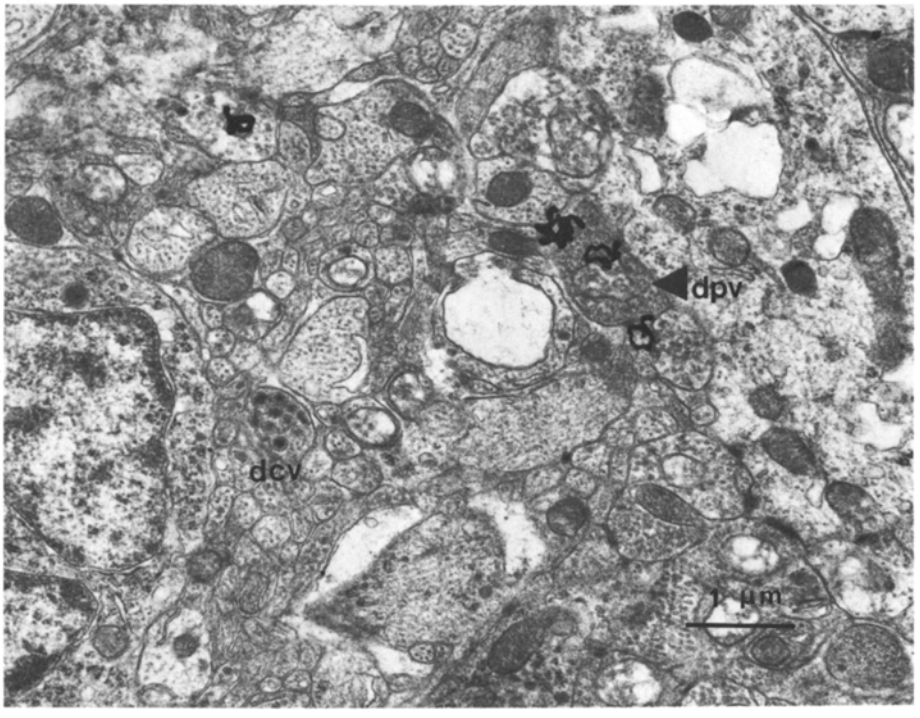

Fig. 9. Electron micrograph from SCvl exhibiting different presynaptic terminals. Contrary to the general observation SG lie above a presynaptic element with closely packed vesicles (*dpv*). Presynaptic elements possessing dense core vesicles (*dcv*) were never associated with SG

Discussion

High resolution photometry was used for the light microscopical evaluation of autoradiographs. The described photometer unit was connected with an off-line magnetic tape station, providing the capacity of the regional computer centre. This unit allows a determination and plotting of relative grain densities over large areas in a short time and relates both with morphological landmarks. Every part of the measured area can be processed for statistical analysis and can therefore establish findings which are not evident by classical methods of microscopy, as can be seen by the rather weak labelling of the contralateral AHN. If no encoding device is needed, the sections can be scanned automatically, thus recording the relative grain densities of 10.000 measurement points together with the corresponding coordinates in less than two hours. Finally, processing of consecutive sections may generate three-dimensional images of parts of interest. The plots and graphs produced by computer-aided analysis of autoradiographs document the high resolution rendered by this method. This resolution is necessary in regions such as the SCA, characterised by striking differences of SG-distribution.

Results obtained with photometric measurements are in close relationship with the actual number of SG underlying the measurement field either in standard preparations or in histological tissue as shown by various authors (Dendy, 1960; Rogers, 1961; Dörmer et al., 1966; Dörmer, 1967).

The measurement-error, engendered by photometry compared with counting individual SG, is allayed by the fact that the relationship between radioactivity applied and incorporated within the tissue studied and the number of developed grains is inaccurately assessed. In addition to physiological parameters affecting amount and distribution of incorporated and axonally transported radioactivity (see Lajtha, 1975) as well as methodological influences during the preparation of the autoradiographs, especially the choice of fixatives and mode of photographic development, various physical conditions also affect the relationship between radioactivity and grain density (Dörmer, 1967; Weibel et al., 1972).

SG counting is limited by the restricted capability to discriminate between single grains either horizontal or vertical to the plane of focus. Even if sophisticated autofocus equipment (Lipkin et al., 1974; Wann et al., 1974) with special time lasting devices and complex SG-analysis algorithms (Entingh and Capowski, 1975) are used, only areas of less than 30% of an elementary layer of SG can be analysed. With photometric measurement there is a linear relationship between the number of grains and the luminous flux to about 70% of the elementary layer (Dörmer, 1967). Therefore, in evaluating autoradiographs for tracing neuronal connectivity, photometric measurement can be undertaken in various parts of the section disregarding extraordinarily high differences in grain concentration as can be seen in Figure 4 where optical grain counting is virtually impossible. The high resolution together with the speed of evaluation and the high storage and processing capacity enable an accumulation of a mass of data necessary for the exact delineation of differentially labelled structures. Moreover, the representation of SG-distribution with the photometric technique permits (but does not require) a matrix display at least one order of magnitude smaller compared with the method developed by Wann et al. (1974).

The plots obtained from animals surviving from 12 h to 30 days showed no obvious changes in grain densities of fibre paths and terminal nuclei, although radioactive label was due to protein transported either by only the rapid or both the rapid and slow axonal flow. Rapidly transported material has been demonstrated to be located predominantly over synaptic terminals (McEwen and Grafstein, 1968; Cowan et al., 1972). Owing to this preference for synaptic terminals and to the slow turnover rate of the rapidly transported material, it can be expected that a shifting of radioactivity takes places in favour of the terminal nuclei (see Droz, 1973; Lajtha, 1975).

The slowly transported material which predominantly labels the axons, does not reach the SCA before the fourth day. To reach the superior colliculi (SC), at least 10 days are necessary in the rat. However, the increased labelling of the SC during this time by rapidly transported material gave no valuable indication at the light microscopic level of a period when terminals (SGS) are labelled in preference to axons (SO).

The obvious differences in the pattern of label distribution within different projection areas were produced by the peculiar arrangement of synaptic terminals. Nuclei receiving optic afferents by synaptic glomerular complexes, such as the LGN, exhibited a strikingly patchy distribution of SG. Structures with uniform synaptic arrangement showed homogeneous labelling. The main part of the SCN was also characterised by the patchy SG-distribution. This would support the

concept of encapsulated synaptic complexes. The homogeneous arrangement of synapses within the contralateral SCvl supports further evidence that this part is cytoarchitectonically different. The labelling of this ventro-lateral area appears much heavier than depicted by other authors, describing optic input to this area (Mai, 1976).

In order to elucidate the question whether these fibres actually terminate in the alleged region, identification of retinal terminals using electron microscopic degeneration techniques appeared insufficient, because interpretations of degenerative changes are unreliable due to artifacts by transneuronal changes following the disintegration of traversing axons (Ghetti et al., 1972).

The thorough observation of the time course of alterations regarding myelinated axons and synaptic profiles as performed by Moore and Lenn (1972) after orbital enucleation of the rat may not rule out entirely that the reported synaptic degeneration was induced by biochemical response of non-optic synapses to the degeneration products. The short interval between the enucleation and the reported structural changes only reflects the intense and rapid reactibility of the injured tissue and emphasises the advantage of the preservation of the functional integrity of neurons by EM-ARG. This method also enabled study of the types of profiles of labelled ganglion cell terminals and may be applied in those cases where selective transsection of fibre paths is impossible.

The fact that dense core vesicles (DCV) were not observed within presynaptic terminals associated with SG further stresses the possibility that the alterations observed by Moore and Lenn (1972), which predominantly affected terminals with DCV, were artifacts.

The fact that the SG were not observed accumulated around a special structure is explained by the extreme thinness of the sections, the short survival time as well as by the structural distribution of synaptic terminals. The area occupied by the total number of synaptic terminals approximates 6 % of the structural components of the SCvl. Only one part of this population can be supposed to be a potential site of axonally transported material. Hendrickson (1972), analysing the SG-distribution within the monkey LGN found one SG per 28 μm^2 evaluated section area after injection of 100–300 μCi ^{3}H-leucine and exposure times up to five months. In this study we found values from 35–40 μm^2 per SG after exposure times between 23 and 26 weeks following injection of 85–135 μCi ^{3}H-leucine. The number of SG per square unit, therefore, is not essentially lower than that reported by Hendrickson (1972) regarding: a) the relatively low number of SG overlying the SCN as compared to the LGN after LM-ARG in the same animal, and b) the total volume of synapses of presumed ganglion cell origin of which approximately half as many are found in the SCN compared with the LGN.

The distribution of SG related with synaptic terminals can not be compared with the cited study or with the results obtained after intracerebral application of ^{3}H-leucine by Dekker and Kuypers (1975). These authors sought to establish the topical relationship between the developed SG and the structures lying within a probability circle of 50 %, whereas we took into consideration the distribution of the percent SG as a function of the distance from the radioactive source within more than one probability are (Bachmann et al., 1968) together with the expected relative density of SG. The different statistical significances between the 66% and

the 90% probability circle (Table 1) support the necessity of weighting the hit structures in regard to the distance from the radioactive source.

Within the observed number of SG a rather high percent must be contributed to the numerous fibres passing through the nucleus as seen in light microscopy. All technical and methodological reservations which could have occurred during the study would further decrease the number of SG related to presynaptic terminals. The preponderance of synaptic labelling as demonstrated in this study therefore confirms beyond doubt that retinal afferents terminate within the evaluated structure.

References

Bachmann, L., Salpeter, M.M., Salpeter, E.E.: Das Auflösungsvermögen elektronenmikroskopischer Autoradiographien. Histochemie **15,** 234–250 (1968)

Bellonici, J.: Über die zentrale Endigung des Nervus opticus bei den Vertebraten. Zeitschr. für wissensch. Zoologie **47,** 1–46 (1888)

Cowan, W.M., Gottlieb, D.I., Hendrickson, A.E., Price, J.L., Woolsey, T.A.: The autoradiographic demonstration of axonal connections in the central nervous system. Brain Res. **37,** 21–51 (1972)

Dekker, J.J., Kuypers, H.G.J.M.: Electron microscopy study of forebrain connections by means of the radioactive labeled amino acid tracer technique. Brain Res. **85,** 229–235 (1975)

Dendy, P.P.: A method for the automatic estimation of grain densities in microautoradiography. Phys. in Med. y Biol. **5,** 131–137 (1960)

Dörmer, P.: Auflichtphotometrische Untersuchungen zur Größe der Koinzidenz in der Autoradiographie mit Tritium. Histochemie **8,** 1–8 (1967)

Dörmer, P.: Photometric methods in quantitative autoradiography. In: Microautoradiography and Electron Probe Analysis (U. Lüttge, ed), pp. 7–48. Berlin-Heidelberg-New York: Springer 1972

Dörmer, P., Brinkmann, W., Stieber, A., Stich, W.: Automatische Silberkornzählung in der Einzelzell-Autoradiographie. Eine neue photometrische Methode für die quantitative Autoradiographie. Klin. Wschr. **44,** 477–482 (1966)

Droz, B.: Renewal of synaptic proteins. Brain Res. **62,** 383–394 (1973)

Entingh, D.J., Capowski, J.J.: Automatic silver grain counting with area accumulation. Automatic Cytology Conference, Asimolar, Calif. (1975)

Ghetti, B., Horoupian, D.S., Wisniewski, H.M.: Transsynaptic response of the lateral geniculate nucleus and the pattern of degeneration of the nerve terminal in the rhesus monkey after eye enucleation. Brain Res. **45,** 31–48 (1972)

Hayhow, W.R., Sefton, A., Webb, C.: Primary optic centers of the rat in relation to the terminal distribution of the crossed and uncrossed optic nerve fibers. J. comp. Neurol. **118,** 295–322 (1962)

Hayhow, W.R., Webb, C., Jervie, A.: The accessory optic fiber system in the rat. J. comp. Neurol. **115,** 187–216 (1960)

Hendrickson, A.E.: Electron microscopic distribution of axoplasmic transport. J. comp. Neurol. **144,** 381–398 (1972)

Kopriwa, B.M., Leblond, C.P.: Improvements in the coating technique of radioautography. J. Histochem. **10,** 269–285 (1962)

Lajtha, A.: Transport and incorporation of amino acids in relation to measurement of axonal flow. In: The Use of Axonal Transport for Studies of Neuronal Connectivity (Cowan, W.M. and M. Cuenod, eds.), pp. 26–45. Amsterdam-Oxford-New York: Elsevier 1975

Lipkin, L.E., Lemkin, P., Carman, G.: Automated autoradiographic grain counting in human determined context. J. Histochem. Cytochem. **22,** 755–765 (1974)

Mai, J.: Quantitative autoradiographische Untersuchungen am subcorticalen optischen System der Albinoratte. Dissertation, Düsseldorf 1976

McEwen, B.S., Grafstein, B.: Rapid transport of labelled material in fish optic nerve. In: Macromolecules and the Function of the Neuron (Z. Lodin and S.P.R. Rose, eds.), pp. 246–255. Proc. of the Internat. Symp. on metabolism of nuclei acids and proteins and the function of the neuron Prag, 1967. Amsterdam: Ex. Medic. Found. 1968

Moore, R.Y., Lenn, N.J.: A retinohypothalamic projection in the rat. J. comp. Neurol. **146,** 1–14 (1972)
Nadler, N.J.: Interpretation of grain counts in electron microscope radioautography. J. Cell Biol. **49,** 877–882 (1971)
Palkovits, M., Zàborszky, L., Ambach, G.: Accessory neurosecretory cell groups in the rat hypothalamus. Acta morph. Acad. Sci. hung. **22** (1), 21–33 (1974)
Rogers, A.W.: A simple photometric device for the quantitation of silver grains in autoradiographs of tissue sections. Exp. Cell. Res. **24,** 228–239 (1961)
Rosenstein, J.M., Leure du Pree, A.E.: Electron microscopic observations of nodes of Ranvier in the external cuneate nucleus. J. comp. Neurol. **170,** 461–484 (1976)
Salpeter, M.M., Bachmann, L.: Autoradiography with the electron microscope. A procedure for improving resolution, sensitivity and contrast. J. Cell Biol. **22,** 469–477 (1964)
Schultz, R.L., Case, N.M.: A modified aldehyde perfusion technique for preventing certain artifacts in electron microscopy of the central nervous system. J. Microsc. **92,** 69–84 (1970)
Venable, J.H., Cogeshall, R.: A simpliefied lead citrate stain for use in electron microscopy. J. Cell Biol. **25,** 405-408 (1965)
Wann, D.F., Price, J.L., Cowan, W.M., Agulnek, M.A.: An automated system for counting silver grains in autoradiographs. Brain Res. **81,** 31–58 (1974)
Weibel, E.R., Fisher, C., Gahm, J., Schaefer, A.: Current capabilities and limitations of available stereological techniques. III. Image analysis with the scanning microphotometer. J. Microsc. **95,** 367–392 (1972)

Accepted May 23, 1977